Mitochondria-Targeted Inhibitors of the Human SIRT3 Lysine Deacetylase

Kathrin S. Troelsen, Michael Bæk, Andreas S. Madsen,† Nima Rajabi, and Christian A. Olsen*

Center for Biopharmaceuticals & Department of Drug Design and Pharmacology, Faculty of Health and Medical Sciences, University of Copenhagen, Universitetsparken 2, DK-2100, Copenhagen, Denmark.

† Present address A.S.M. is now at Novo Nordisk A/S, DK-2880, Bagsværd, Denmark.

*cao@sund.ku.dk

ABSTRACT

Sirtuin 3 (SIRT3) is the major protein lysine deacetylase in the mitochondria. This hydrolase regulates a wide range of metabolically involved enzymes and has been considered as a potential drug target in certain cancers. Investigation of pharmacological intervention has been challenging due to a lack of potent and selective inhibitors of SIRT3. Here, we developed a strategy for selective inhibition of SIRT3 in cells, over its structurally similar isozymes that localize primarily to nucleus (SIRT1) and cytoplasm (SIRT2). This was achieved by directing the inhibitors straight to the mitochondria through incorporation of sequences inspired by previously described mitochondria-targeting peptides. Our inhibitors exhibited excellent mitochondrial localization in HeLa cells as indicated by fluorophore-conjugated versions and target engagement was demonstrated by a thermal shift assay of SIRT3 using western blotting. The acetylation state of documented SIRT3 target MnSOD was shown to be perturbed in cells with little effect on known targets of SIRT1 and SIRT2, showing that our lead compound exhibits selectivity for SIRT3 in cells. We expect that the developed inhibitor will now enable a more detailed investigation of SIRT3 as a potential drug target and help shed further light on the diverse biology regulated by this enzyme.

Keywords: Sirtuins, SIRT3, histone deacetylase inhibitors, mitochondrial targeting, cell penetrating peptides

Introduction

The sirtuin (SIRT) enzymes are evolutionarily conserved hydrolases of the class III lysine deacetylases (KDACs), cleaving acyl-based posttranslational modifications (PTMs) on lysine side chains in the proteome. The human genome encodes seven sirtuin isoforms, SIRT1–7, which have different substrate specificities, cellular localization, and tissue-dependent expression levels.[1] The major deacetylases [i.e., targeting the ε-*N*-acetyllysine (Kac) PTM] are SIRT1–3, SIRT6, and SIRT7, of which the class I sirtuins, SIRT1–3, share the highest similarity in substrate specificity.[2-3] Thus, SIRT1–3 efficiently hydrolyze Kac residues as well as longer hydrocarbon-based *ε-N*-acyllysine PTMs such as *ε-N*-myristoyllysine (Kmyr)[4-6] to regulate diverse biological function, including metabolic homeostasis and healthspan.[7] However, the class I sirtuins have also been implicated in the pathogenesis of various diseases and, depending on the condition, either activation or inhibition of SIRT1–3 has been considered as potential therapeutic strategies to treat several cancers and neurodegenerative disorders.[8-10] The SIRT3 isoform is the only mitochondrially localized sirtuin that exhibits potent deacetylase activity, with other mitochondrial sirtuins, SIRT4 and SIRT5, mainly targeting negatively charged PTMs.[11-17] Here, SIRT3 regulates a number of metabolic enzymes involved in the respiratory chain,[18] TCA cycle,[19-20] fatty acid β-oxidation,[21] and ketogenesis.[22] Furthermore, it controls mitochondrial oxidative pathways by regulating the production of reactive oxygen species (ROS),[23] e.g. through activation of manganese superoxide dismutase (MnSOD).[24-25]

The sirtuins share a common deacylase mechanism, which is dependent on the co-substrate nicotinamide adenine dinucleotide (NAD^+). This mechanism has been utilized to develop so-called mechanism-based inhibitors, by the use of substrate-mimicking chemotypes that form stalled intermediates in the active site of the sirtuin.[26-33] Many mechanism-based inhibitors exhibit high potency and, in several cases, high selectivity toward specific sirtuin subtypes. However, due to the shared mechanism and similar substrate preferences between SIRT1–3, it has been difficult to target SIRT3 selectively. Therefore, we envisioned adopting a strategy to achieve selective targeting of the enzyme through specific subcellular localization of the inhibitor, rather than solely relying on selective enzyme recognition. Among several demonstrated examples of mitochondrial targeting of various payloads,[34] a particularly appealing approach for our strategy was the mitochondria-targeting peptides developed by Kelley and co-workers.[35-37] Based on recent investigations of mechanism-based peptide inhibitors of other sirtuins,[30, 33] we hypothesized that mitochondria-targeting peptide tags could be elaborated into potent inhibitors of the SIRT3 that would exhibit selectivity in cells (Figure 1). By designing such chemotypes and optimizing their selectivity profiles to target SIRT1–3 equipotently, while not inhibiting other sirtuins or class I HDACs, we could indeed demonstrate

selective inhibition of SIRT3 in cultured cells as well as target engagement illustrated by cellular thermal shift assays.

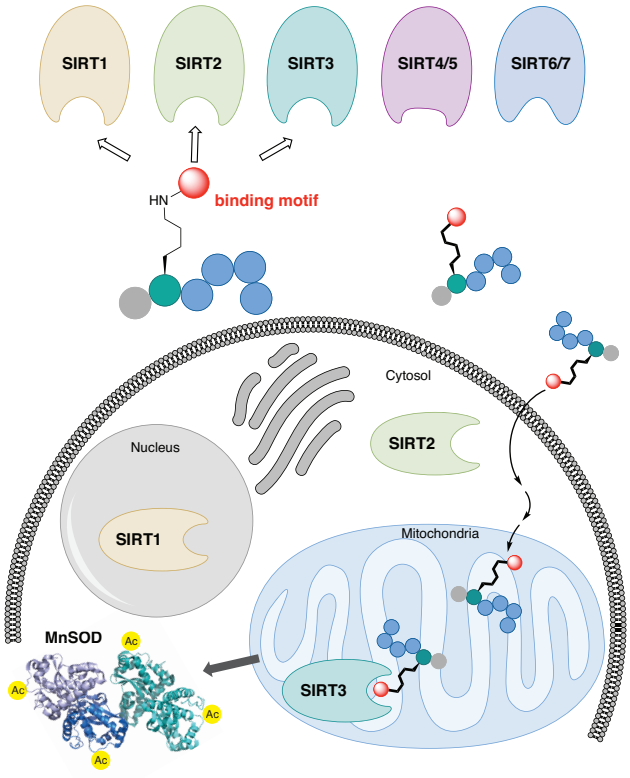

Figure 1. Schematic representation of the developed concept for inhibition of SIRT3. A potent inhibitor that exhibit class I sirtuin selectivity, targeting SIRT1–3, is targeted to the mitochondria to inhibit SIRT3 selectively in cells by localization.

Results and Discussion

Structure–activity relationship study

We envisioned that the mitochondrial targeting peptides developed by Kelley and co-workers[35-37] could be starting points for mechanism-based inhibitors of sirtuins. It was hypothesized that such inhibitors could be designed by incorporating a modified lysine residue that would enable sirtuin inhibition. Based on insight from previous structure–activity relationship (SAR) studies targeting SIRT2 and SIRT5, including selectivity screenings and co-crystal structures,[30, 33] we positioned the ADP-ribose-binding thiocarbonyl-containing lysine residue as the N-terminal amino acid (see Scheme S1 and S2 for syntheses). First, we addressed the effect of mitochondria-targeting peptide length combined with ε-*N*-thioacetylation or ε-*N*-thiomyristoylation of the N-terminal lysine residue. The inhibitors were evaluated for their ability to inhibit the deacetylation activities of SIRT1–3 at two doses, applying previously described fluorescence-based assay protocols.[12, 38] Gratifyingly, this

revealed that the peptide scaffolds allowed for potent inhibition of SIRT1–3 (Figure S1). Based on this initial compound series, the thiomyristoylated analogs were abandoned due to their apparent selectivity towards SIRT2. An analog of the pentamer peptide was also synthesized with alternation of the hydrophobic and cationic residues, resulting in slight selectivity for SIRT1, which was not considered optimal either (Figure S1). Next, we compared five *ε-N*-thioacetyllysine analogs – based on the best pentapeptide sequence – containing different N-terminal functional groups (Figure S2). The substituents were selected based on previous SAR and supporting X-ray co-crystal structures. Those studies indicated a high degree of freedom for the selection of functionalities at this position and that potency is substantially more reliant on inhibitor backbone–enzyme interactions.[30, 33] Based on this series, we decided to proceed with the 3-phenylpropionyl group (**c**; Figure 2) and the alkyne-containing group (**a**, Figure 2), which is amenable for incorporation of fluorophores or other tags using Cu(I)-catalyzed azide–alkyne Huisgen 3+2 cycloaddition "click" chemistry.[39-40] Inspired by previous studies of SIRT1–3[27, 33, 41-45] and the structures of the active sites in SIRT1–3 (Figure S3), we analyzed a number of binding motifs using the trimeric scaffold with the "clickable" N-terminal modification (**1**–**10**; Figure 2A). The most potent inhibitors of SIRT3 were compounds **1**, **4**, and **6**, with **1** and **4** showing the lowest degree of off-target inhibition of SIRT1 and 2 (Figure 2B). However, because ε-*N*-thioacetyllysine residues have been shown to be processed by HDAC8[46] and SIRT1–3,[43] the *ε-N'*-methylthiourea functionality was chosen for further investigations.

Satisfied that potent inhibition of SIRT3 could be achieved with compound **4** without significant selectivity towards either SIRT1 or SIRT2 (Figure S3,4), we synthesized fluorophore-containing analogs (**11**, **13**, and **16**) to address mitochondrial targeting. Additionally, 3-phenylpropionyl-containing analogs (**14** and **17**) were synthesized to address in-cell activity of the inhibitors. In addition to the nitrobenzoxadiazole (NBD, **b**) fluorophore, we also prepared analogs containing Abz (**18**), BODIPY, ATTO, and EDANS (see Scheme S2B for structures). Before analyzing the mitochondrial targeting ability of the fluorophore-containing analogs we demonstrated excellent stability of selected inhibitors in DMEM cell culture medium (Figure S6). Additionally, toxicity was evaluated for selected compounds against a series of immortalized cell lines (Figure S7 and Table S2) to inform us about appropriate dosing during the cellular fluorescence experiments.

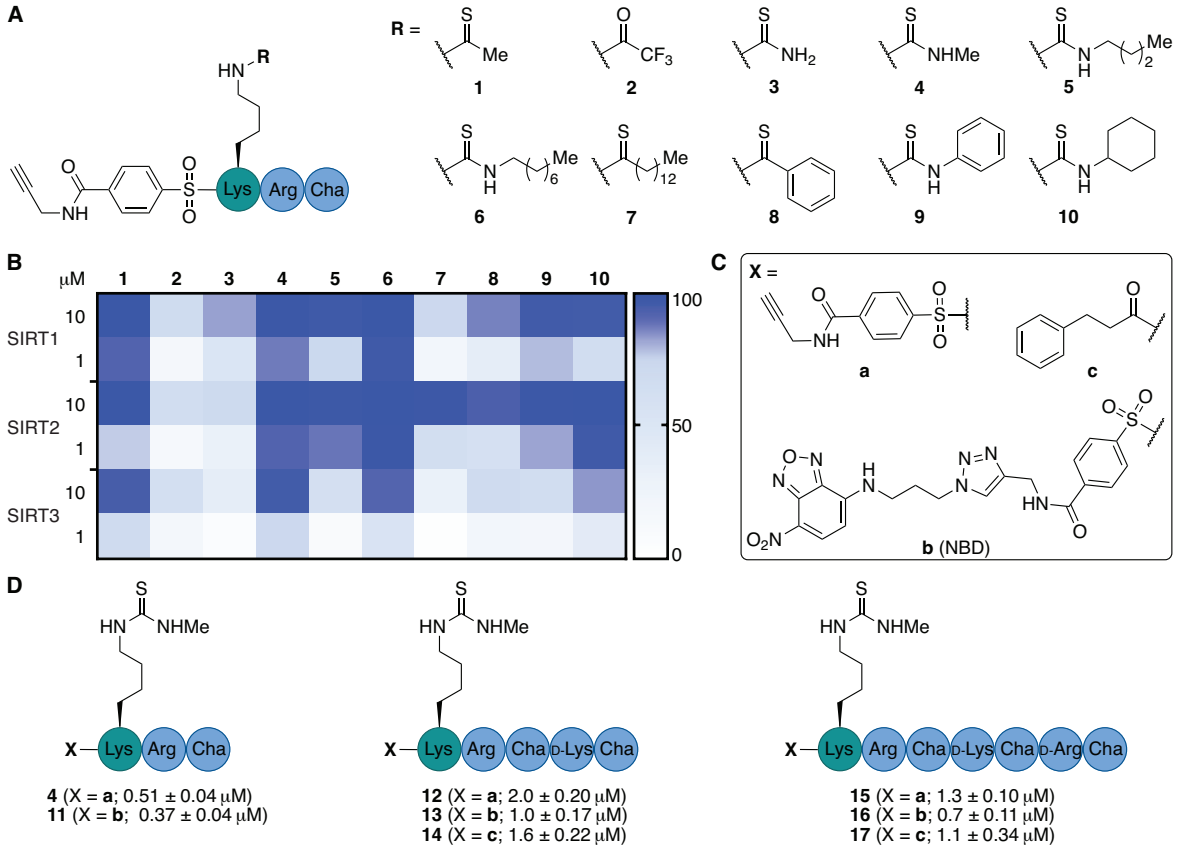

Figure 2. Structure–activity relationship of inhibitors against SIRT1–3. (A) Structures of compounds 1–10. (B) Heatmap summarizing potencies of compounds **1**–**10** against SIRT1–3 based on %-inhibition. All assays were performed at least twice in duplicate and the values can be found in Table S1. (C) Structures of N-terminal functional groups introduced in compounds **11**–**17**. (D) Structures and IC_{50} values and standard deviations recorded for compounds **11**–**17** based on a minimum of two individual assays performed in duplicate. Further information can be found in Figure S5 and Table S1.

Mitochondrial localization

The cellular localization of compounds **11**, **13**, and **16** was first evaluated in Hela cells (Figure 3 and Figure S8). Not surprisingly, the trimeric scaffold **11** did not display satisfactory cellular or mitochondrial uptake (Figure 3A), which is in line with a previous report where tetramers were the smallest motifs shown to induce mitochondrial targeting.[35] Both the pentameric (**13**) and heptameric (**16**) probes were taken up by the cells and showed excellent overlap with the MitoTracker™ co-staining dye (Figure 3B,C). However, a significant fraction of the cells in the population seemed perturbed by the longer inhibitor (**16**), and all three NBD-conjugated inhibitors were bleaching extremely fast, making the analysis challenging. We therefore investigated the heptameric inhibitor using a selection of alternative fluorophores, chosen based on their reported bleaching properties, size, charge, and commercial availability. The aim being to identify a fluorophore with better performance, which could be readily incorporated without altering the properties of the inhibitor too

drastically. Unfortunately, poor cellular uptake was observed for the ATTO-containing analog (**S11**) (Figure S8). Similarly, the EDANS-conjugated analog (**S13**) showed low permeability, perhaps due to the negative charge present in this fluorophore (Figure S8).

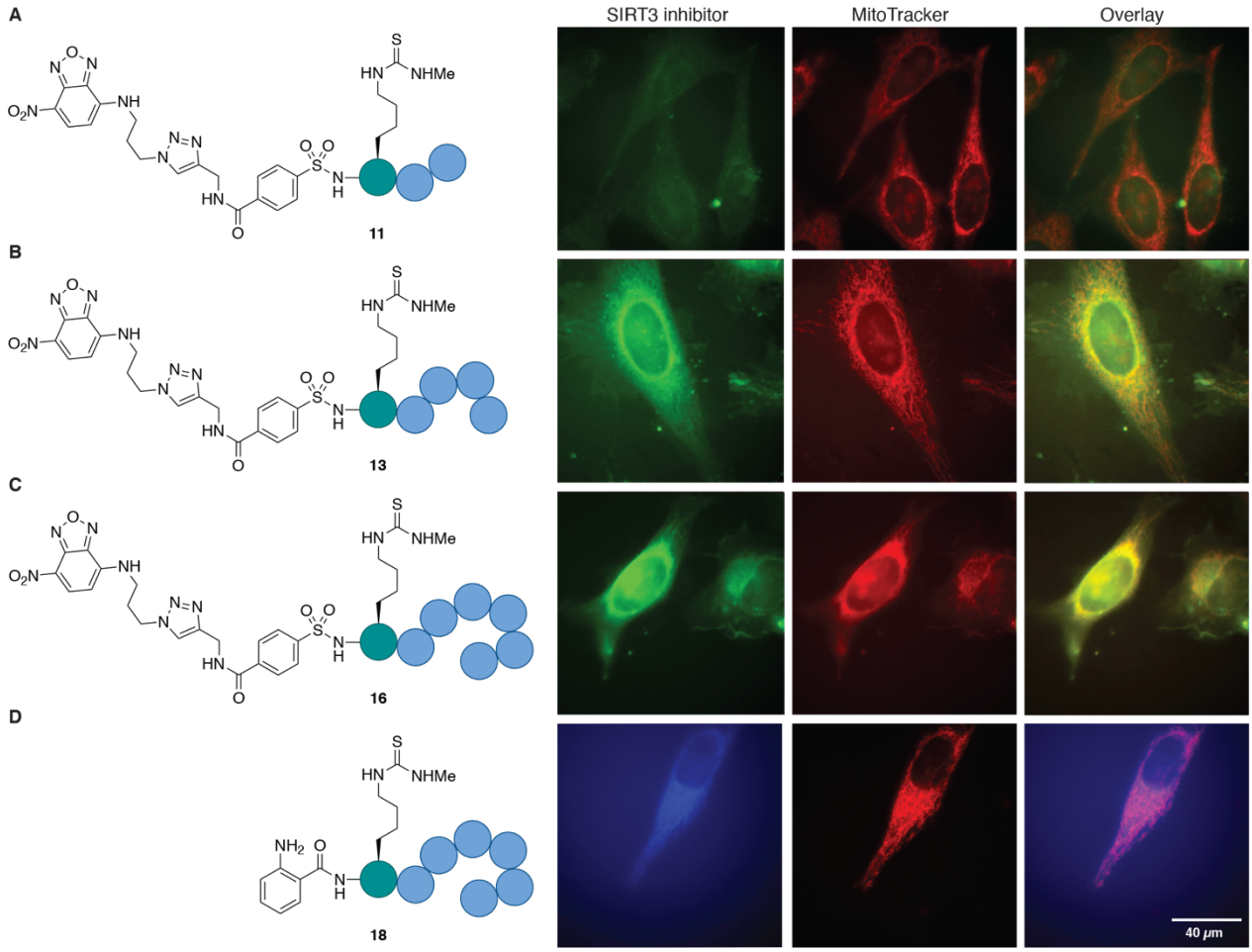

Figure 3. Mitochondrial targeting of fluorophore labeled inhibitors in HeLa cells, determined by co-staining with MitoTracker™. (A) NBD-labeled trimer (**11**); Pearson correlation coefficient (r) = –0.66. (B) NBD-labeled pentamer (**13**); Pearson correlation coefficient (r) = 0.59. (C) NBD-labeled heptamer (**16**); Pearson correlation coefficient (r) = 0.46. (D) Abz-labeled heptamer (**18**); Pearson correlation coefficient (r) = 0.81.

An analog containing the widely used BODIPY fluorophore (**S12**) exhibited excellent photostability and good mitochondrial targeting as judged by the co-localization with MitoTracker dye (Figure S8). However, significant perturbation of a large fraction of the cells was observed, including vesicle formation, possibly through disruption of the mitochondria. Finally, 2-aminobenzoyl (Abz), which offers a minimal structural modification of the inhibitor due to its small size, was introduced to give compound **18**. Although this fluorophore is less powerful with a quantum yield of 0.6 for the free

acid,[47] compared to 0.94 for BODIPY,[48] it exhibited clear cellular uptake and did show overlap with the MitoTracker dye, indicating mitochondrial targeting of compound **18** (Figure 2).

Brightfield images indicated primarily healthy Hela cells after treatment with most fluorophore-conjugated (Figure S8) as well as the non-fluorophore-conjugated compounds (**14** and **17**; Figure S9). However, slightly increased toxicity was observed for the heptameric scaffolds and substantial changes to the cell morphology were visible for the BODIPY-conjugated compound as also indicated by the fluorescence images discussed above. As expected, the control peptide NBD-TAT was distributed evenly within the cells with no significant co-localization to the mitochondria and no indication of toxicity in the brightfield images (Figure S8).

Taken together, the data strongly suggest that our inhibitors, based on both pentameric and heptameric mitochondrial targeting peptides, are indeed shuttled to the mitochondria in HeLa cells in culture.

Targeting of SIRT3 in HEK293T cells in culture

With the compounds based on the longer heptapeptide mitochondria-targeting sequence showing convincing localization to the mitochondria, we were interested in investigating whether SIRT3 was indeed inhibited selectively in cells. Cellular studies were performed with the non-fluorophore conjugated compound (**17**), due to its low cytotoxicity against HEK293T, HeLa, Jurkat, and MCF-7 cells (GI_{50} values >10 μM) (Figure S7 and Table S2), its low perturbation of cells according to brightfield microscopic images of treated HeLa cells (Figure S9), as well as its stability in growth medium (Figure S6). First, we chose the documented mitochondrial protein target MnSOD, for which the degree of acetylation of lysine 68 (K68) has been shown to be regulated by SIRT3.[24-25, 49-50] Inspired by the work of Meier and co-workers on non-enzymatic acylation,[51] we developed a novel mitochondrial targeting acetylating agent (**NR-E65**) to be used as a positive control (see Scheme S3 for structure). Gratifyingly, **NR-E65** showed a significant increase in MnSOD (K68) acetylation in mitochondria-enriched HEK293T lysates. Similarly, cells treated with compound **17** showed a significant increase in MnSOD (K68) acetylation, using 10 μM of the inhibitor (Figure 4A,B, Figure S10, and Figure S11). To further substantiate that compound **17** is targeting SIRT3 in living cells, we performed cellular thermal shift assays, using western blot (Figure 4C,D and Figure S12).[52-53] Analysis of the normalized data led to a statistically significant shift in thermal stability compared to the DMSO control (Figure 4D), strongly suggesting target engagement of compound **17** with SIRT3 in HEK293T cells in culture.

Finally, we addressed whether the targeting of SIRT3 was also selective over SIRT1 and 2 in HEK293T cells. For SIRT1, we chose the well documented target p53[45, 54-55] and analyzed the levels

of acetylated p53 (K382) in HEK293T cells treated with compound **17**, using the known SIRT1 inhibitors **EX-527**[56] and **19**[31, 43] as positive controls (Figure 4E,F and Figure S13). Although, compounds **17**, **EX-527**, and **19** are equipotent against SIRT1 *in vitro*,[43] the effect on p53 acetylation (K382) by compound **17** is significantly lower than the positive control compounds (Figure 4E,F), suggesting a high degree of selectivity for SIRT3 over SIRT1 in cells.

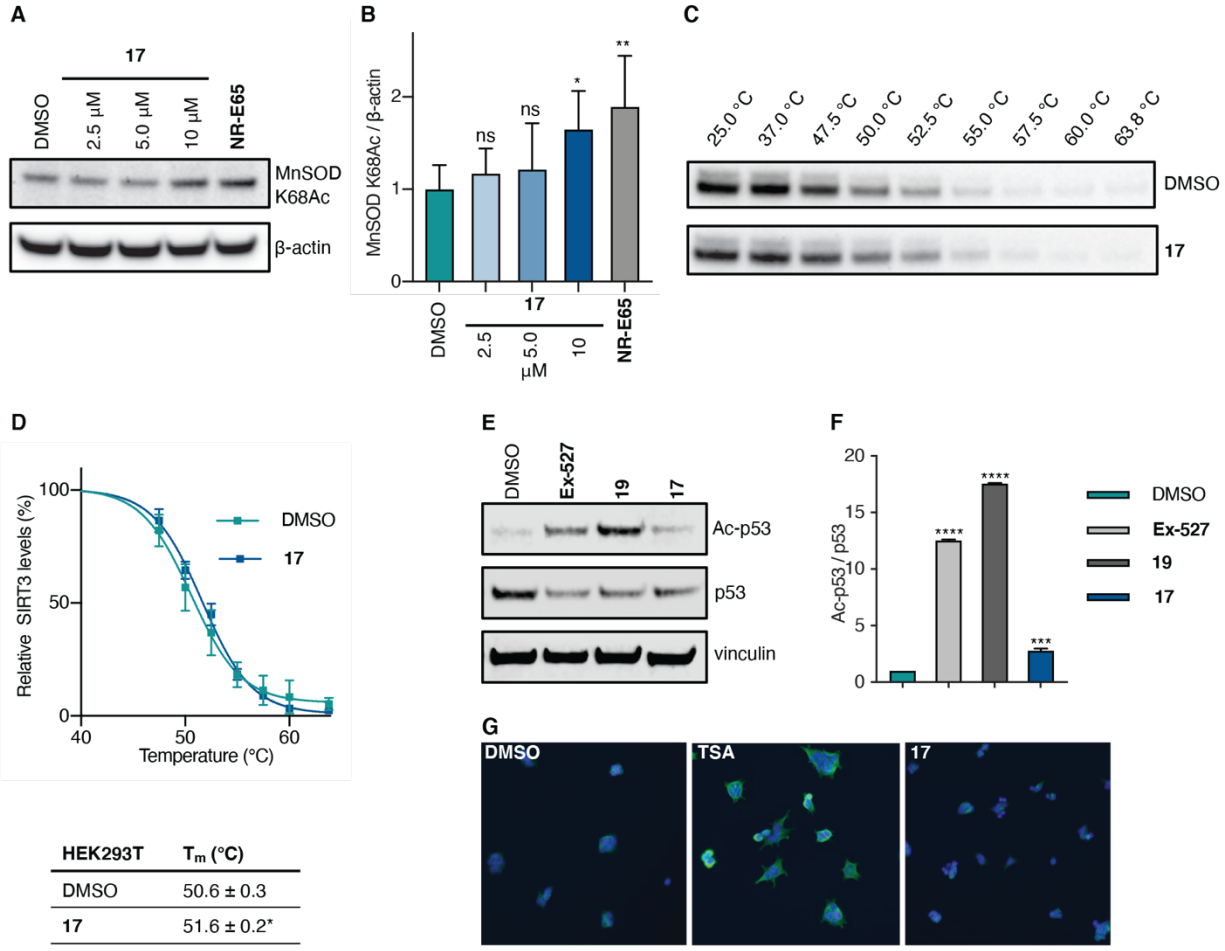

HEK293T	T_m (°C)
DMSO	50.6 ± 0.3
17	51.6 ± 0.2*

Figure 4. Inhibition of SIRT3 in HEK293T cells. (A) Western blot showing dose-dependent effect of **17** on acetylation of documented mitochondrial SIRT3 target MnSOD. (B) Quantification and statistics of the effect on MnSOD acetylation, based on three individual experiments performed at least in duplicate. (C) Western blot of the cellular thermal shift effect of treatment with **17** on SIRT3 stability. (D) Analysis of the quantification of the bands from the cellular thermal shift assay. (E) Evaluation of off-target effect of **17** (25 μM) on p53 acetylation compared to positive controls **Ex-527** (25 μM) and **19** (25 μM) by western blot. (F) Quantification and statistics of the effect on p53 acetylation (K40). (G) Immunofluorescence investigation of the effect of **17** (25 μM) on α-tubulin acetylation compared to TSA (1 μM) as the positive control. Additional data, full gel images, and structures of **NR-E65**, **Ex-527**, **19**, and **TSA** are available in the Supporting Information Scheme S3 and Figures S8–S14. Significance of the CETSA shifts were calculated using unpaired t-test of T_m values from independent experiments. Adjusted P-values ns $P > 0.05$, *$P < 0.05$, **$P < 0.01$ compared to DMSO treated control. Significance of the levels of Ac-p53 and MnSOD K68Ac were calculated using one way ANOVA test. Adjusted P-values ns $P > 0.05$, *$P < 0.05$, **$P < 0.01$, ***$P < 0.001$, ****$P < 0.0001$ compared to DMSO treated control.

For SIRT2, we and others have recently reported on the challenges of determining cellular effects on lysine acetylation by performing western blots on whole cell extracts.[22,57] We therefore investigated the effect of **17**, as well as the shorter analog **14**, on α-tubulin acetylation (K40) qualitatively by performing immunofluorescence experiments, comparing to DMSO and TSA as negative and positive controls, respectively (Figure 4G and Figure S14). While treatment with TSA produced a significant increase in α-tubulin acetylation compared to the DMSO control, no change was observed when treating cells with either compound **14** or **17**, indicating high selectivity towards SIRT3 over SIRT2 in cells as well.

Taken together, the limited degree of SIRT1,2 inhibition in cells further substantiates the mitochondrial targeting properties of our non-fluorophore-conjugated inhibitors, which effectively inhibit SIRT3 in cells.

Conclusion

It has been a major challenge to develop inhibitors that selectively perturb SIRT3 of the class I sirtuin enzymes. Due to the high structural similarity of the active sites of SIRT1–3, small molecule chemotypes have largely failed in producing selective inhibition of SIRT3 over SIRT1 and 2. The differences in the structures of the extended substrate-binding pockets among these three enzymes have enabled the development of selective inhibitors of SIRT2, but have not been successfully harnessed to target SIRT1 or SIRT3. Here, we developed compounds based on a different strategy that takes advantage of the differential sub-cellular localization of the three class I sirtuins. In work reported during the finalization of our study, a commonly used mitochondrial targeting motif (the triphenylphosphonium group) was attached to a SIRT2 inhibitor, to inhibit SIRT3 in the mitochondria rather than SIRT1 and SIRT2 in the nucleus and cytosol, respectively.[58] The chemotypes developed in the present study, however, have a fundamentally different architecture and includes optimization of their selectivity profiles to dial down affinity for SIRT1 and SIRT2. Our design was predicated on the fusion of attributes from mechanism-based class I sirtuin inhibitors with mitochondria-targeting peptides. After succeeding in the achievement of potent enzyme inhibition *in vitro*, we optimized of mitochondria-targeting properties and secured compound stability together with limited toxicity. The resulting probe compound exhibited direct engagement of SIRT3 in the mitochondria of cells in culture by an inhibitor molecule for the first time and the acetylation level of the documented SIRT3 target MnSOD was perturbed.

We expect that this novel probe will enable investigation of the function of SIRT3 with unprecedented precision and thus help uncover the potential for development of future therapeutics targeting this enzyme. Finally, our results provide a framework that may be exploited for the targeting of other

mitochondrial proteins, including the mitochondrial sirtuin isoforms, SIRT4 and SIRT5, by incorporating alternative acyl group mimics that are selectively targeted by these enzymes.

ORCID

Kathrin Sten Troelsen: 0000-0002-8734-533X

Michael Bæk: 0000-0001-7416-9421

Nima Rajabi: 0000-0002-9509-7540

Christian Adam Olsen: 0000-0002-2953-8942

Conflict of interest

The authors declare no conflict of interest.

Acknowledgements

We thank Alexander L. Nielsen for donation of building blocks and control compounds and Julie E. Bolding for assistance with mitochondrial enrichment and donation of recombinant SIRT7. This work was supported by the Lundbeck foundation (PhD Fellowship grant R218-2016-1277 and Running Cost grant R289-2018-2074t), the Danish Independent Research Council–Natural Sciences (Grant No. 6108-00166B), the Carlsberg Foundation (2013-01-0333, CF15-011, and CF18-0442), the Novo Nordisk Foundation (NNF17OC0029464), and the European Research Council (ERC-CoG-725172–*SIRFUNCT*).

References

[1] M. C. Haigis, D. A. Sinclair, *Annu. Rev. Pathol.: Mech. Dis.* **2010**, *5*, 253-295.
[2] A. Chalkiadaki, L. Guarente, *Nat. Rev. Cancer* **2015**, *15*, 608-624.
[3] N. Rajabi, I. Galleano, A. S. Madsen, C. A. Olsen, in *Progress in Molecular Biology and Translational Science, Vol. 154* (Ed.: W. Zheng), Academic Press, **2018**, pp. 25-69.
[4] H. Jiang, S. Khan, Y. Wang, G. Charron, B. He, C. Sebastian, J. Du, R. Kim, E. Ge, R. Mostoslavsky, H. C. Hang, Q. Hao, H. Lin, *Nature* **2013**, *496*, 110.
[5] J. L. Feldman, J. Baeza, J. M. Denu, *J. Biol. Chem.* **2013**, *288*, 31350-31356.
[6] A. S. Madsen, C. Andersen, M. Daoud, K. A. Anderson, J. S. Laursen, S. Chakladar, F. K. Huynh, A. R. Colaço, D. S. Backos, P. Fristrup, M. D. Hirschey, C. A. Olsen, *J. Biol. Chem.* **2016**, *291*, 7128-7141.
[7] R. H. Houtkooper, E. Pirinen, J. Auwerx, *Nature Rev. Mol. Cell Biol.* **2012**, *13*, 225.
[8] M. Schiedel, D. Robaa, T. Rumpf, W. Sippl, M. Jung, *Med. Res. Rev.* **2018**, *38*, 147-200.
[9] M. S. Bonkowski, D. A. Sinclair, *Nature Rev. Mol. Cell Biol.* **2016**, *17*, 679-690.
[10] Y. Jiang, J. Liu, D. Chen, L. Yan, W. Zheng, *Trends Pharmacol Sci.* **2017**, *38*, 459-472.
[11] J. Du, Y. Zhou, X. Su, J. J. Yu, S. Khan, H. Jiang, J. Kim, J. Woo, J. H. Kim, B. H. Choi, B. He, W. Chen, S. Zhang, R. A. Cerione, J. Auwerx, Q. Hao, H. Lin, *Science* **2011**, *334*, 806.
[12] A. S. Madsen, C. A. Olsen, *J. Med. Chem.* **2012**, *55*, 5582-5590.
[13] K. A. Anderson, F. K. Huynh, K. Fisher-Wellman, J. D. Stuart, B. S. Peterson, J. D. Douros, G. R. Wagner, J. W. Thompson, A. S. Madsen, M. F. Green, R. M. Sivley, O. R. Ilkayeva, R.

D. Stevens, D. S. Backos, J. A. Capra, C. A. Olsen, J. E. Campbell, D. M. Muoio, P. A. Grimsrud, M. D. Hirschey, *Cell Metab.* **2017**, *25*, 838-855.
[14] M. Pannek, Z. Simic, M. Fuszard, M. Meleshin, D. Rotili, A. Mai, M. Schutkowski, C. Steegborn, *Nat. Comm.* **2017**, *8*, 1513.
[15] M. Tan, C. Peng, K. A. Anderson, P. Chhoy, Z. Xie, L. Dai, J. Park, Y. Chen, H. Huang, Y. Zhang, J. Ro, G. R. Wagner, M. F. Green, A. S. Madsen, J. Schmiesing, B. S. Peterson, G. Xu, O. R. Ilkayeva, M. J. Muehlbauer, T. Braulke, C. Muhlhausen, D. S. Backos, C. A. Olsen, P. J. McGuire, S. D. Pletcher, D. B. Lombard, M. D. Hirschey, Y. Zhao, *Cell Metab.* **2014**, *19*, 605-617.
[16] C. Roessler, C. Tuting, M. Meleshin, C. Steegborn, M. Schutkowski, *J. Med. Chem.* **2015**, *58*, 7217-7223.
[17] C. Roessler, T. Nowak, M. Pannek, M. Gertz, G. T. Nguyen, M. Scharfe, I. Born, W. Sippl, C. Steegborn, M. Schutkowski, *Angew. Chem. Int. Ed.* **2014**, *53*, 10728-10732.
[18] B. H. Ahn, H. S. Kim, S. Song, I. H. Lee, J. Liu, A. Vassilopoulos, C. X. Deng, T. Finkel, *Proc. Natl. Acad. Sci. U. S. A.* **2008**, *105*, 14447-14452.
[19] C. Schlicker, M. Gertz, P. Papatheodorou, B. Kachholz, C. F. Becker, C. Steegborn, *J. Mol. Biol.* **2008**, *382*, 790-801.
[20] H. Cimen, M. J. Han, Y. Yang, Q. Tong, H. Koc, E. C. Koc, *Biochemistry* **2010**, *49*, 304-311.
[21] M. D. Hirschey, T. Shimazu, E. Goetzman, E. Jing, B. Schwer, D. B. Lombard, C. A. Grueter, C. Harris, S. Biddinger, O. R. Ilkayeva, R. D. Stevens, Y. Li, A. K. Saha, N. B. Ruderman, J. R. Bain, C. B. Newgard, R. V. Farese Jr, F. W. Alt, C. R. Kahn, E. Verdin, *Nature* **2010**, *464*, 121.
[22] T. Shimazu, M. D. Hirschey, L. Hua, K. E. Dittenhafer-Reed, B. Schwer, D. B. Lombard, Y. Li, J. Bunkenborg, F. W. Alt, J. M. Denu, M. P. Jacobson, E. Verdin, *Cell Metab.* **2010**, *12*, 654-661.
[23] A. S. Bause, M. C. Haigis, *Exp. Gerontol.* **2013**, *48*, 634-639.
[24] X. Qiu, K. Brown, M. D. Hirschey, E. Verdin, D. Chen, *Cell Metab.* **2010**, *12*, 662-667.
[25] R. Tao, M. C. Coleman, J. D. Pennington, O. Ozden, S.-H. Park, H. Jiang, H.-S. Kim, C. R. Flynn, S. Hill, W. Hayes McDonald, A. K. Olivier, D. R. Spitz, D. Gius, *Mol. Cell* **2010**, *40*, 893-904.
[26] B. M. Hirsch, C. A. Gallo, Z. Du, Z. Wang, W. Zheng, *MedChemComm* **2010**, *1*, 233-238.
[27] B. C. Smith, J. M. Denu, *Biochemistry* **2007**, *46*, 14478-14486.
[28] B. C. Smith, J. M. Denu, *J. Biol. Chem.* **2007**, *282*, 37256-37265.
[29] B. C. Dancy, S. A. Ming, R. Papazyan, C. A. Jelinek, A. Majumdar, Y. Sun, B. M. Dancy, W. J. Drury, 3rd, R. J. Cotter, S. D. Taverna, P. A. Cole, *J. Am. Chem. Soc.* **2012**, *134*, 5138-5148.
[30] N. Rajabi, M. Auth, K. R. Troelsen, M. Pannek, D. P. Bhatt, M. Fontenas, M. D. Hirschey, C. Steegborn, A. S. Madsen, C. A. Olsen, *Angew. Chem. Int. Ed.* **2017**, *56*, 14836-14841.
[31] S. V. Olesen, N. Rajabi, B. Svensson, C. A. Olsen, A. S. Madsen, *Biochemistry* **2018**, *57*, 3903-3915.
[32] M. Bæk, P. Martín-Gago, J. S. Laursen, J. L. H. Madsen, S. Chakladar, C. A. Olsen, *Chem.–Eur. J.* **2020**, *26*, 3862-3869.
[33] A. L. Nielsen, N. Rajabi, N. Kudo, K. L. Larsen, M. Fontenas, A. Lucidi, A. S. Madsen, M. Yoshida, C. A. Olsen, *(bioRxiv 2020, DOI: 10.1101/2020.03.20.000380*.
[34] M.-C. Frantz, P. Wipf, *Environmental and Molecular Mutagenesis* **2010**, *51*, 462-475.
[35] K. L. Horton, K. M. Stewart, S. B. Fonseca, Q. Guo, S. O. Kelley, *Chem. Biol.* **2008**, *15*, 375-382.
[36] L. F. Yousif, K. M. Stewart, S. O. Kelley, *ChemBioChem* **2009**, *10*, 1939-1950.
[37] K. L. Horton, M. P. Pereira, K. M. Stewart, S. B. Fonseca, S. O. Kelley, *ChemBioChem* **2012**, *13*, 476-485.
[38] D. Wegener, F. Wirsching, D. Riester, A. Schwienhorst, *Chem. Biol.* **2003**, *10*, 61-68.
[39] C. W. Tornoe, C. Christensen, M. Meldal, *J. Org. Chem.* **2002**, *67*, 3057-3064.

[40] V. V. Rostovtsev, L. G. Green, V. V. Fokin, K. B. Sharpless, *Angew. Chem. Int. Ed.* **2002**, *41*, 2596-2599.
[41] J. L. Feldman, K. E. Dittenhafer-Reed, N. Kudo, J. N. Thelen, A. Ito, M. Yoshida, J. M. Denu, *Biochemistry* **2015**, *54*, 3037-3050.
[42] X. Bao, Y. Wang, X. Li, X.-M. Li, Z. Liu, T. Yang, C. F. Wong, J. Zhang, Q. Hao, X. D. Li, *eLife* **2014**, *3*, e02999.
[43] N. Rajabi, A. L. Nielsen, C. A. Olsen, *ACS Med. Chem. Lett.* **2020***, doi: 10.1021/acsmedchemlett.9b00580*
[44] B. Chen, J. Wang, Y. Huang, W. Zheng, *Bioorg. Med. Chem. Lett.* **2015**, *25*, 3481-3487.
[45] H. Jing, J. Hu, B. He, Y. L. Negrón Abril, J. Stupinski, K. Weiser, M. Carbonaro, Y.-L. Chiang, T. Southard, P. Giannakakou, R. S. Weiss, H. Lin, *Cancer Cell* **2016**, *29*, 297-310.
[46] M. Zessin, Z. Kutil, M. Meleshin, Z. Novakova, E. Ghazy, D. Kalbas, M. Marek, C. Romier, W. Sippl, C. Barinka, M. Schutkowski, *Biochemistry* **2019**, *58*, 4777-4789.
[47] A. S. Culf, H. Yin, S. Monro, A. Ghosh, D. A. Barnett, R. J. Ouellette, M. Cuperlovic-Culf, S. A. McFarland, *Bioorg. Med. Chem.* **2016**, *24*, 929-937.
[48] L. D. Lavis, R. T. Raines, *ACS Chem. Biol.* **2008**, *3*, 142-155.
[49] Y. Chen, J. Zhang, Y. Lin, Q. Lei, K.-L. Guan, S. Zhao, Y. Xiong, *EMBO Reports* **2011**, *12*, 534-541.
[50] C. He, J. M. Danes, P. C. Hart, Y. Zhu, Y. Huang, A. L. de Abreu, J. O'Brien, A. J. Mathison, B. Tang, J. M. Frasor, L. M. Wakefield, D. Ganini, E. Stauder, J. Zielonka, B. N. Gantner, R. A. Urrutia, D. Gius, M. G. Bonini, *Proc. Natl. Acad. Sci. U. S. A.* **2019**.
[51] R. A. Kulkarni, A. J. Worth, T. T. Zengeya, J. H. Shrimp, J. M. Garlick, A. M. Roberts, D. C. Montgomery, C. Sourbier, B. K. Gibbs, C. Mesaros, Y. C. Tsai, S. Das, K. C. Chan, M. Zhou, T. Andresson, A. M. Weissman, W. M. Linehan, I. A. Blair, N. W. Snyder, J. L. Meier, *Cell Chem. Biol.* **2017**, *24*, 231-242.
[52] D. Martinez Molina, R. Jafari, M. Ignatushchenko, T. Seki, E. A. Larsson, C. Dan, L. Sreekumar, Y. Cao, P. Nordlund, *Science* **2013**, *341*, 84-87.
[53] D. Martinez Molina, P. Nordlund, *Annu. Rev. Pharmacol. Toxicol.* **2016**, *56*, 141-161.
[54] T. Suzuki, T. Asaba, E. Imai, H. Tsumoto, H. Nakagawa, N. Miyata, *Bioorg. Med. Chem. Lett.* **2009**, *19*, 5670-5672.
[55] H. Vaziri, S. K. Dessain, E. N. Eaton, S.-I. Imai, R. A. Frye, T. K. Pandita, L. Guarente, R. A. Weinberg, *Cell* **2001**, *107*, 149-159.
[56] A. D. Napper, J. Hixon, T. McDonagh, K. Keavey, J. F. Pons, J. Barker, W. T. Yau, P. Amouzegh, A. Flegg, E. Hamelin, R. J. Thomas, M. Kates, S. Jones, M. A. Navia, J. O. Saunders, P. S. DiStefano, R. Curtis, *J. Med. Chem.* **2005**, *48*, 8045-8054.
[57] T. Rumpf, M. Schiedel, B. Karaman, C. Roessler, B. J. North, A. Lehotzky, J. Oláh, K. I. Ladwein, K. Schmidtkunz, M. Gajer, M. Pannek, C. Steegborn, D. A. Sinclair, S. Gerhardt, J. Ovádi, M. Schutkowski, W. Sippl, O. Einsle, M. Jung, *Nat. Commun.* **2015**, *6*.
[58] M. Li, Y. L. Chiang, C. A. Lyssiotis, M. R. Teater, J. Y. Hong, H. Shen, L. Wang, J. Hu, H. Jing, Z. Chen, N. Jain, C. Duy, S. J. Mistry, L. Cerchietti, J. R. Cross, L. C. Cantley, M. R. Green, H. Lin, A. M. Melnick, *Cancer Cell* **2019**, *35*, 916-931.

ToC Graphic

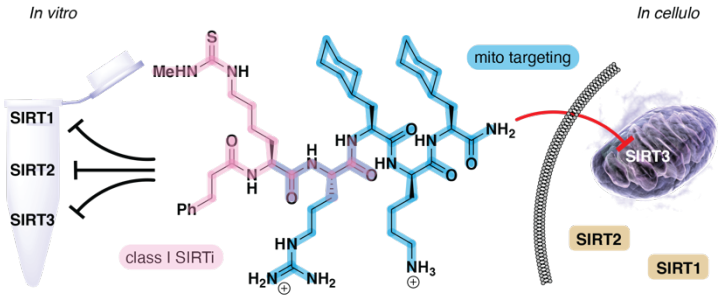
In vitro
In cellulo
SIRT1
SIRT2
SIRT3
class I SIRTi
mito targeting
SIRT3
SIRT2
SIRT1